Hannah S. Pulferer and Gernot R. Müller-Putz*

Continuous error processing during a closed-loop 2D tracking task

https://doi.org/10.1515/cdbme-2022-1045

Abstract: The usefulness of error-related potentials (ErrPs) for control in non-invasive Brain-Computer interface (BCI) research has been established over the last decades. To continuously correct for erroneous action of an end effector (e.g., robot arm) in a BCI however, these neural correlates relating only to the discrete perception of errors remain problematic. Using a pre-recorded dataset offering feedback in a 2D tracking task in different correct or erroneous conditions, we analyzed whether error processing during continuous feedback can be observed from the electroencephalogram (EEG). Within this dataset comprising 30 sessions of recordings, we were able to detect significant differences between correct and erroneous conditions. Furthermore, minimal significant difference between two erroneous conditions is reported, confirming the direct connection between error and cognitive response.

Keywords: Electroencephalography (EEG), continuous error processing, continuous 2D target tracking, brain-computer interface (BCI)

1 Introduction

In the early 1990, the existence of a neural correlate in electroencephalographic (EEG) signals to the perception of errors was first established [1, 2]. This correlate, the Error-related Potential (ErrP), is characterized consecutively by a peak in fronto-central negativity and parietal positivity, which appear shortly after an erroneous event is perceived. As decoded signals within a brain-computer interface (BCI), especially within motor decoding, remain erroneous, BCI research has been utilizing ErrPs to identify erroneous action (e.g., of an end effector) as an interaction error in the EEG and correct accordingly [3]. However, apart from varying considerably with age [4], the neurophysiology of the ErrP was additionally shown to modulate strongly with the level of attention the erroneous event receives, as well as with the significance that is attributed to the error by the participant [5, 6]. Especially the latter has led to the necessity of limiting the number of erroneous trials in EEG studies to ensure the detection of an ErrP, which however cannot readily be translated to everyday situations. The exploration of neural correlates to continuously detected errors may provide a solution to this problem [7, 8]. In this work, we analyzed a previously recorded dataset comprising EEG recordings during the perception of correct, slightly erroneous and severely erroneous continuous feedback within a 2D tracking task. We hypothesized that significant differences should be visible between correct and erroneous conditions, while minimal distinction between slight and severe error condition should be observed. Here, we present the results of a time series analysis in two different frequency bands, providing further evidence that non-discrete errors can be detected from the EEG during continuous tasks as well.

***Corresponding author: Gernot R. Müller-Putz,**
Institute of Neural Engineering, Stremayrgasse 16/IV, Graz Austria
BioTechMed Graz, Austria
e-mail: gernot.mueller@tugraz.at
Hannah S. Pulferer, Institute of Neural Engineering, Graz, Austria

2 Methods

2.1 Dataset and recording

Data of a prior study were used [9], comprising recordings (60 channel EEG according to the 10-10 system, four channel electrooculogram (EOG), sampling rate 200Hz) of ten right-handed, non-disabled participants within three sessions each, amounting to a total of 30 sessions of recordings. For the following analysis, data of calibration snakeruns, 50% and 100% EEG feedback snakeruns were used.

2.2 Paradigm and setup

Within each session, the participants were asked to track a moving target (white snake; Fig.1a-c) on a TV screen visually, as well as via attempted movement of their dominant arm as if controlling a computer mouse. An encasing around the limb akin to [10] (see Fig.1f) prevented overt movement. Simultaneously, feedback (red dot, Fig.1a-c) was depicted to visualize the current performance.

2.3 Conditions

Each session was divided into an offline calibration part, followed by online runs of varying feedback conditions. During calibration, fake feedback in the form of a slightly delayed

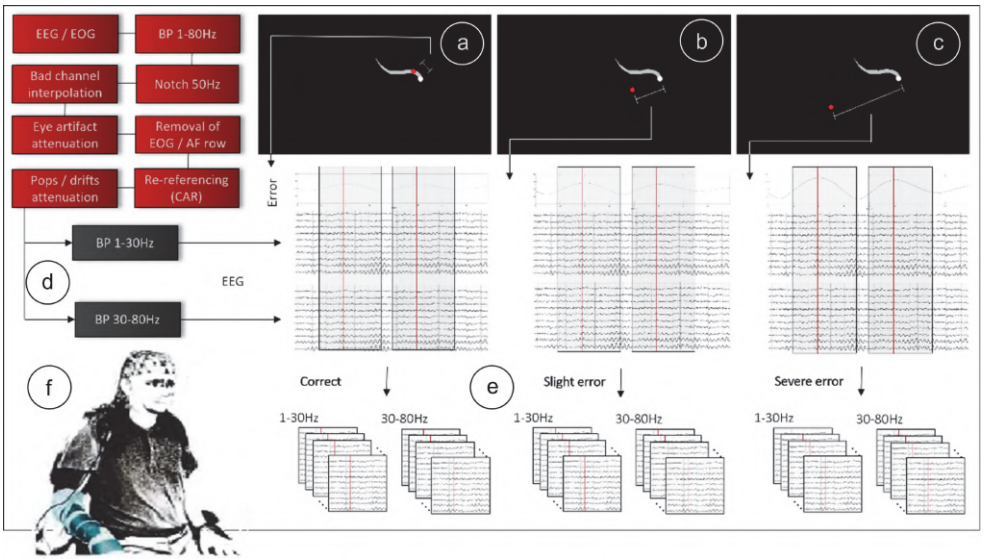

Fig. 1: Processing pipeline and analysis scheme. Depicted target (white snake) and feedback (red dot) during **(a)** Correct, **(b)** Slight Error and **(c)** Severe Error conditions. Data processed as shown in **(d)** and band-pass filtered between 1-30Hz and 30-80Hz was finally epoched to windows of [-1, 3]s within the local maximum of the Euclidean error between feedback and snake **(e)**. Setup with the participant's dominant arm strapped to the chair to mimic attempted movement **(f)**.

snake was depicted to accustom the participants to the feedback dot as data (48 trials) were recorded to calibrate the trajectory decoder [11–13] (Fig.1a). Aside from this delay, the feedback largely coincided with the target, implying that no error processing was induced during the calibration runs. Epochs of calibration data are thus henceforth labelled *Correct*. Within the online part of the measurement, ongoing EEG signals were used to infer the aspired position on screen, which was depicted as real-time feedback via feedback dot. To facilitate the transition from fake to real (erroneous) feedback, only 50% of the EEG-decoded positional information was first used (36 trials, henceforth *Slight Error*), before 100% EEG-decoded information (36 trials, henceforth *Severe Error*) was depicted. As the delivered feedback deviated considerably from the target with increasing EEG information, we hypothesized that error processing had to be happening during both online conditions.

2.4 Data processing

Data of EEG and EOG were band-pass filtered between 1-80Hz, line noise was removed, and bad channels were interpolated. Eye artifacts were attenuated using SGEYESUB [14], followed by the removal of EOG and AF row electrodes. Data were re-referenced to common average reference, pops and drifts were removed using the HEAR algorithm [15]. From here, data were band-pass filtered between 1-30Hz and 30-80Hz, following the line of previous work which reported delta to beta bands [16–18], as well as subbands of the gamma [19] to carry relevant information during error processing. Next, the Euclidean error between target position (see Fig.1a-c, snake) and decoded position (red dot) was calculated for each condition (Correct, Slight Error, Severe Error). Afterwards, the EEG signals were time-locked to the local maxima of the Euclidean error and sliced into epochs lasting from 1s prior until 3s after an error maximum as shown in Fig.1e.

3 Results

Significant differences between correct and both erroneous conditions in each frequency band (1-30Hz, 30-80Hz) were assessed via a permutation paired t-test. Corrections for multiple comparisons relating to timepoints (801), channels (55), pairwise comparison between the possible conditions (3) and observed frequency bands (2) were made using FDR correction at a significance level of 0.05 [20]. For the high frequency band (30-80Hz), no significant differences in the time series within any pair of conditions could be observed.

The results for the low frequency band (1-30Hz) are shown in Fig.2. The grand average Euclidean error in pixels within the epoched time frames for all three conditions is shown in Fig.2a. Results of the pairwise comparisons between conditions are shown in Fig.2b-d (Correct vs. Slight Error, Correct vs. Severe Error, and Slight Error vs. Severe Error). The upper plot (red, bright/dark gray) always corresponds to the grand average signals at the electrode FCz (red diamond in the sensor plot, top left corner), the lower plot (blue, bright/dark gray) to the grand average signals at Pz (blue diamond in the sensor plot). Topoplots below each comparison show significant areas in the difference (non-significant areas shaded light grey). Shaded areas around the signals denote the standard error of the mean (SEM), shaded rectangular light gray areas denote timepoints of significant difference in the respective channel. The timepoint corresponding to the local maximum of the Eu-

clidean error (t=0ms) is marked with a red vertical line.
For both comparisons of Correct vs. Error (Fig.2b,c, topoplots), significant differences in the patterns are seen throughout the duration of the epoch, with a strong frontal negativity around 0-250ms, followed by a parietal positivity between 500-750ms. In general, the difference signals (Correct-Error; red/blue signals) appear modulated by the Euclidean error (Fig.2a), with peaks in negativity at FCz (red) following shortly after an error maximum, peaks in positivity at Pz (blue) appearing at a negative slope of the error.
Comparing the two different error conditions (Slight Error vs. Severe Error, Fig.2d), a significant difference in the patterns is only seen around 750ms (topoplots, Fig.2d). For the channel FCz, significant difference is only observed at 750ms (Fig.2d, top). At Pz, short timeframes of significant differences are shown between 500ms and 1000ms (Fig.2d, bottom).
For all conditions, grand average signals between approximately -0.5µV and 0.5µV are seen, wherein the parietal amplitude of the erroneous conditions is attenuated, the frontocentral amplitude is increased compared to the correct condition.

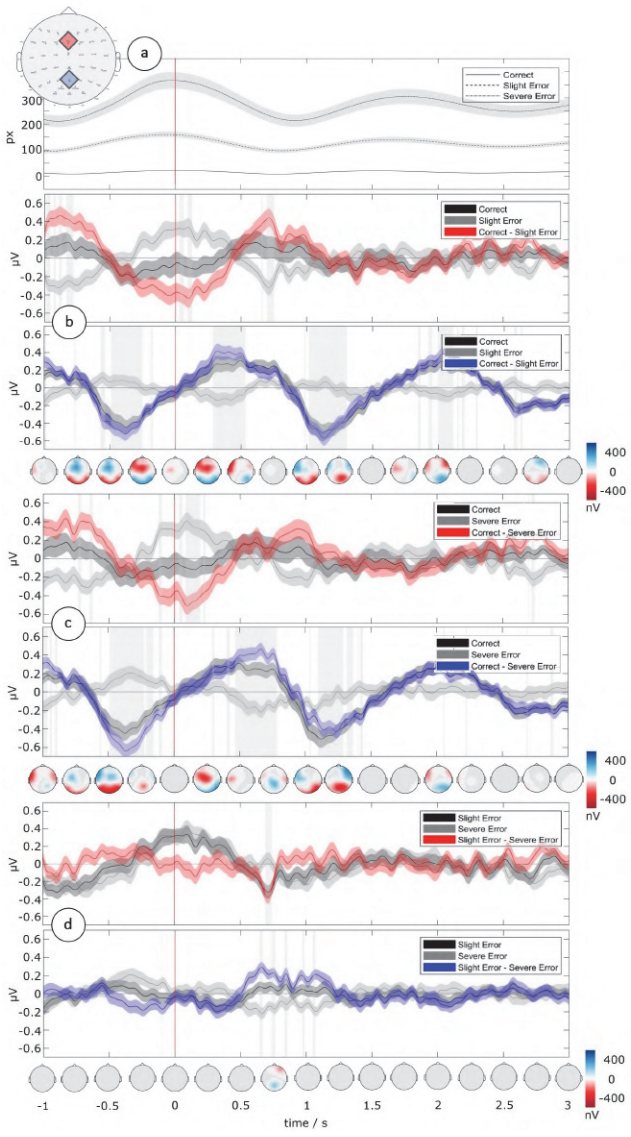

Fig. 2: Grand average Euclidean error for all conditions and electrode layout with selected channels FCz (red) and Pz (blue) **(a)**. Grand average signals at FCz (red, bright/dark gray - top) and Pz (blue, bright/dark gray - bottom) with statistically significant activations (topoplots) for Correct vs. Slight Error **(b)**, Correct vs. Severe Error **(c)** and Slight Error vs. Severe Error **(d)** comparisons. (For visualization, EEG signals above were band-pass filtered between 1-10Hz.)

4 Discussion and Conclusion

Within EEG recordings of ten different participants in a total of 30 sessions, we investigated differences between epochs of correct and epochs of erroneous feedback in two different frequency bands (1-30Hz and 30-80Hz).
We observed significant differences in the lower regarded frequency band, in line with previous works reporting delta and theta [16], alpha [17] and beta [18] as informative bands. We could not observe significant differences in the gamma band (30-80Hz) time domain within any pair of conditions.
For the 1-30Hz band, in which significant differences were observed, we showed the results of three different pairwise comparisons (Fig.2b-d): Correct vs. (Slight/Severe) Error and Slight Error vs. Severe Error. As hypothesized, we were able to observe significant differences between correct and erroneous epochs across the whole epoch length, with modulations in the difference signals at FCz and Pz (red/blue curves in Fig.2b, c) according to the behavior of the Euclidean error (Fig.2a). In contrast, aside from significant differences at around 750ms (topoplot Fig.2d), no significant differences can be reported between the two erroneous conditions. Especially the signals recorded at FCz, an electrode position usually consulted within error processing studies due to its location above the anterior cingulate cortex [21], exhibit no significant differences apart from around 750ms (Fig.2d, top), confirming that the reported results are in fact directly related to a cortical response to the erroneous feedback.
Nevertheless, further analysis of responses related to discrete errors compared to the observed responses reported here needs to be done. Although we see a similar characteristic as observed within an Outcome ErrP [7], both amplitude and latency of the signals differ considerably from classical ErrPs and further emphasize the discrepancy between the mental processing of discrete and continuously appearing erroneous

events. Additionally, time-frequency analysis remains to be done specifically in the gamma band, as differences not observable within the time series of the signals may be found for continuous error processing as well, as reported before by [19], who found significant differences between correct and erroneous conditions especially for the 70-80Hz subband of the gamma when investigating the spectral power. And finally, source space analysis, and specifically, connectivity analysis between selected cortical regions of interest may yield additional insights on how continuous feedback information is processed in the brain.

Author Statement

Authors state no conflict of interest. Informed consent has been obtained from all individuals included in this study. The measurements were conducted as a part of the 'Feel Your Reach' project and as such were approved by the ethics committee of the Medical University of Graz (votum number 32-583 ex 19/20). This research was supported by funding from the European Research Council (ERC-CoG 2015 681231'Feel Your Reach') and NTU-TUG joint PhD program.

References

[1] M. Falkenstein, J. Hohnsbein, J. Hoormann, and L. Blanke, "Effects of crossmodal divided attention on late ERP components. II. Error processing in choice reaction tasks," Electroencephalogr. Clin. Neurophysiol., vol. 78, no. 6, pp. 447–455, Jun. 1991.

[2] W. J. Gehring, B. Goss, M. G. H. Coles, D. E. Meyer, and E. Donchin, "A Neural System for Error Detection and Compensation," Psychol. Sci., vol. 4, no. 6, pp. 385–390, Nov. 1993.

[3] R. Chavarriaga, A. Sobolewski, and J. D. R. Millán, "Errare machinale est: the use of error-related potentials in brain-machine interfaces," Front. Neurosci., vol. 8, p. 208, Jul. 2014.

[4] M. Falkenstein, J. Hoormann, and J. Hohnsbein, "Changes of error-related ERPs with age," Exp. Brain Res., vol. 138, no. 2, pp. 258–262, May 2001.

[5] G. Hajcak, J. S. Moser, N. Yeung, and R. F. Simons, "On the ERN and the significance of errors," Psychophysiology, vol. 42, no. 2, pp. 151–160, Mar. 2005.

[6] C. Lopes-Dias, A. I. Sburlea, and G. R. Müller-Putz, "Masked and unmasked error-related potentials during continuous control and feedback," J. Neural Eng., vol. 15, no. 3, p. 036031, Apr. 2018.

[7] M. Spüler and C. Niethammer, "Error-related potentials during continuous feedback: using EEG to detect errors of different type and severity," Front. Hum. Neurosci., vol. 9, p. 155, Mar. 2015.

[8] C. Lopes-Dias, A. I. Sburlea, and G. R. Müller-Putz, "Online asynchronous decoding of error-related potentials during the continuous control of a robot," Sci Rep 9, 17596, 2019. https://doi.org/10.1038/s41598-019-54109-x

[9] H. S. Pulferer, B. Ásgeirsdóttir, V. Mondini, A. I. Sburlea, and G. R. Müller-Putz, "Continuous 2D trajectory decoding from attempted movement: across-session performance in able-bodied and feasibility in a spinal cord injured participant," J. Neural Eng., 2022. https://doi.org/10.1088/1741-2552/ac689f

[10] M. Velliste, S. Perel, M. C. Spalding, A. S. Whitford, and A. B. Schwartz, "Cortical control of a prosthetic arm for self-feeding," Nature, vol. 453, no. 7198, pp. 1098–1101, May 2008.

[11] V. Mondini, R. J. Kobler, A. I. Sburlea, and G. R. Müller-Putz, "Continuous low-frequency EEG decoding of arm movement for closed-loop, natural control of a robotic arm," J. Neural Eng., vol. 17, no. 4, p. 046031, Aug. 2020.

[12] R. J. Kobler, A. I. Sburlea, V. Mondini, M. Hirata, and G. R. Müller-Putz, "Distance- and speed-informed kinematics decoding improves M/EEG based upper-limb movement decoder accuracy," J. Neural Eng., vol. 17, no. 5, p. 056027, Nov. 2020.

[13] V. Martínez-Cagigal, R. J. Kobler, V. Mondini, R. Hornero, and G. R. Muller-Putz, "Non-linear online low-frequency EEG decoding of arm movements during a pursuit tracking task," in 2020 42nd Annual International Conference of the IEEE Engineering in Medicine Biology Society (EMBC), 2020, pp. 2981–2985.

[14] R. J. Kobler, A. I. Sburlea, C. Lopes-Dias, A. Schwarz, M. Hirata, and G. R. Müller-Putz, "Corneo-retinal-dipole and eyelid-related eye artifacts can be corrected offline and online in electroencephalographic and magnetoencephalographic signals," Neuroimage, vol. 218, p. 117000, Sep. 2020.

[15] R. Kobler, A. I. Sburlea, V. Mondini, and G. Müller-Putz, "HEAR to remove pops and drifts: the high-variance electrode artifact removal (HEAR) algorithm," in Proceedings of the 41th Annual International Conference of the IEEE Engineering in Medicine and Biology Society (EMBC), IEEE Xplore, 2019.

[16] J. Yordanova, M. Falkenstein, J. Hohnsbein, and V. Kolev, "Parallel systems of error processing in the brain," Neuroimage, vol. 22, no. 2, pp. 590–602, Jun. 2004.

[17] J. Carp and R. J. Compton, "Alpha power is influenced by performance errors," Psychophysiology, vol. 46, no. 2, pp. 336–343, Mar. 2009.

[18] T. Koelewijn, H. T. van Schie, H. Bekkering, R. Oostenveld, and O. Jensen, "Motor-cortical beta oscillations are modulated by correctness of observed action," Neuroimage, vol. 40, no. 2, pp. 767–775, Apr. 2008.

[19] M. Völker et al., "The dynamics of error processing in the human brain as reflected by high-gamma activity in noninvasive and intracranial EEG," Neuroimage, vol. 173, pp. 564–579, Jun. 2018.

[20] Y. Benjamini and Y. Hochberg, "Controlling the false discovery rate: A practical and powerful approach to multiple testing," J. R. Stat. Soc., vol. 57, no. 1, pp. 289–300, Jan. 1995.

[21] R. Iannaccone, T. U. Hauser, P. Staempfli, S. Walitza, D. Brandeis, and S. Brem, "Conflict monitoring and error processing: new insights from simultaneous EEG-fMRI," Neuroimage, vol. 105, pp. 395–407, Jan. 2015.